

Supplementary Information for
A Dual-Benefit Flash Pyrolysis for Valorizing Carbonaceous
Wastes into High-Calorific Syngas (94.7% Combustibles)
and Battery Anodes

Pengfei Huang ^[a,b], Li Chen ^[a], Zekun Li ^[a], Zhedong Liu ^[a], Wei-Di Liu ^[c], Jingchao Zhang ^[a],

Jiawei Luo ^[a], Wenjun Zhang ^[b], Xinxin Zhang ^[b], Rongtao Zhu* ^[b], Yanan Chen* ^[a]

^[a] School of Materials Science and Engineering, Key Laboratory of Advanced Ceramics,

Machining Technology of Ministry of Education, Tianjin Key Laboratory of Composite and

Functional Materials, Tianjin University, Tianjin, 300072 China

^[b] Key Laboratory of Coal Processing and Efficient Utilization of Ministry of Education, China

University of Mining and Technology, Xuzhou 221116, Jiangsu, China

^[c] School of Chemistry and Physics, ARC Research Hub in Zero-emission Power Generation for

Carbon Neutrality, and Centre for Materials Science, Queensland University of Technology;

Brisbane, 4000, Australia

* Corresponding author. Tel: +86-755-86244014

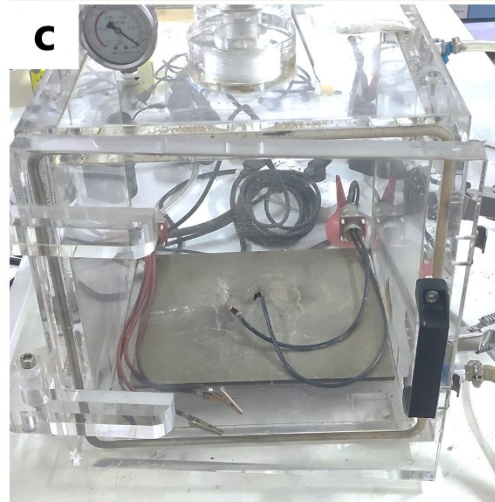
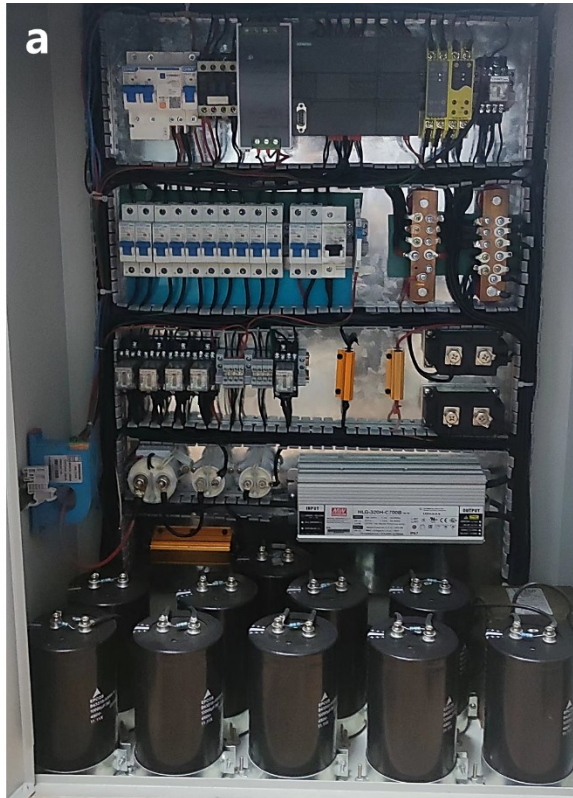
E-mail address: yananchen@tju.edu.cn (Y. chen); rtzhu2010@cumt.edu.cn (R. Zhu)

Keyword: Ultra-High Temperature; Flash Pyrolysis; Non-Equilibrium state; Hydrogen Production; Reducing CO₂ Emissions.

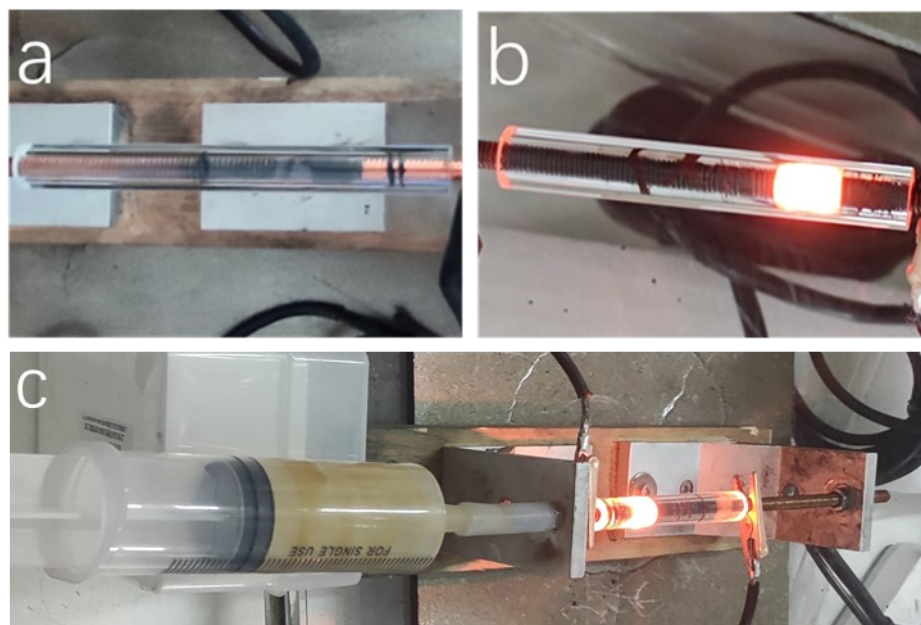
This PDF file includes:

1. Supplementary Figures S1-11
2. Supplementary Tables S1-S2

Supplementary Figure S 1. Schematic diagram of the experimental setup

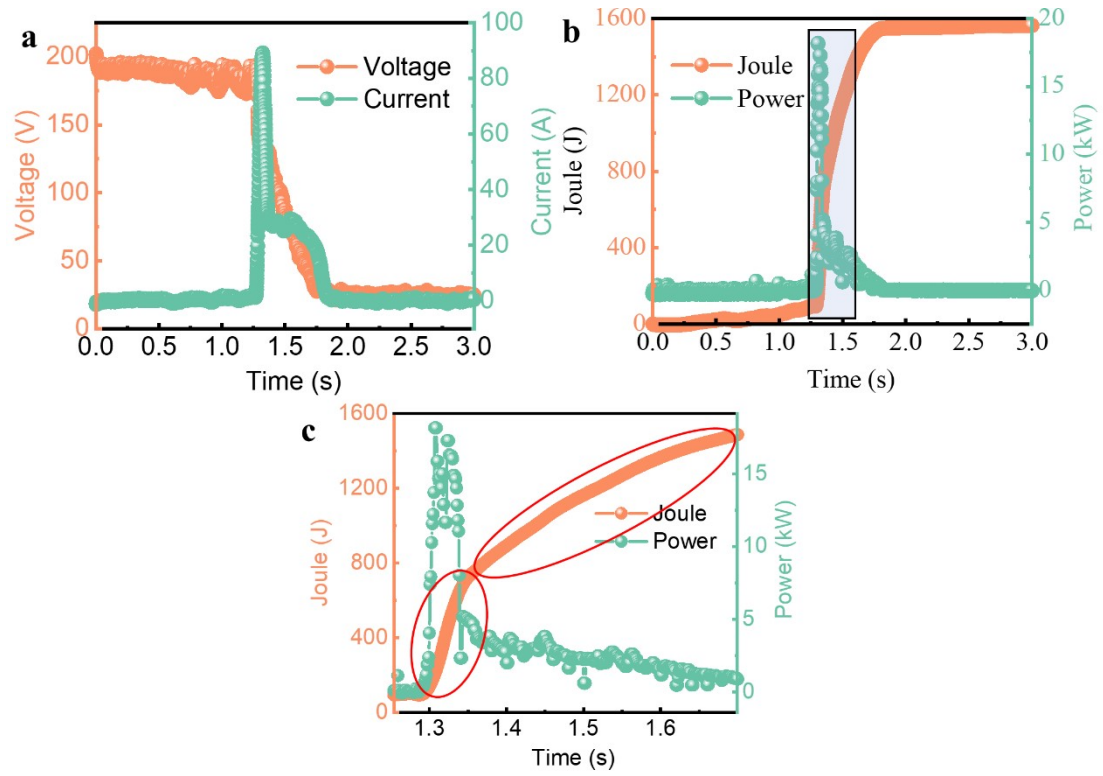


Supplementary Figure S 2. Optical photos before and after the Flash Joule Heating (FJH) reaction

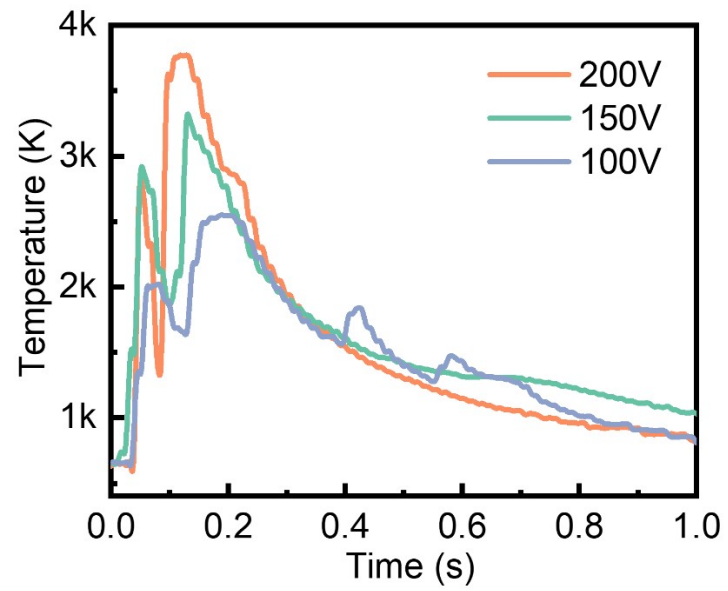


Device schematic: A quartz tube, measuring 10 cm in length, with an inner diameter of 6 mm and a wall thickness of 3 mm, is utilized. Copper electrodes, each with a diameter of 6 mm, are positioned at both tube ends. One end features a gas hollow electrode linked to a gas collection device. The sample is positioned between these electrodes. O-ring seals are incorporated into the electrodes to prevent gas leakage during the Flash Joule Heating (FJH) process.

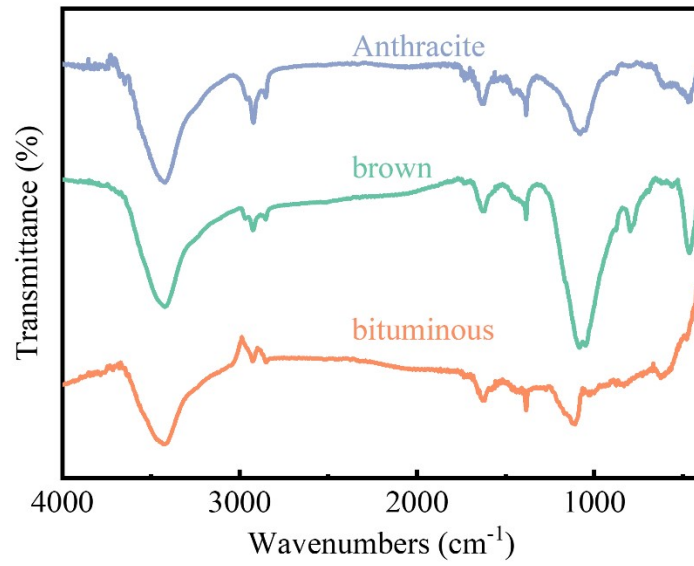
Supplementary Figure S 3. Electrical signal parameters



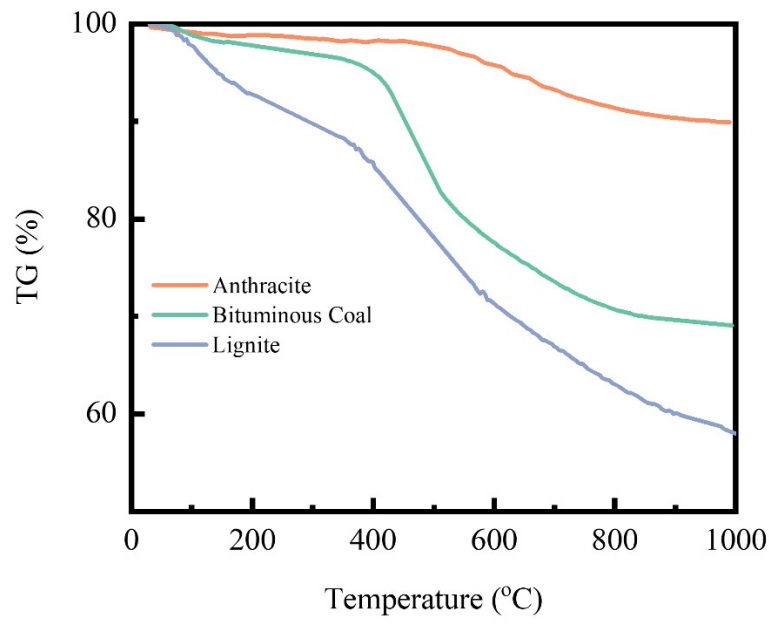
Supplementary Figure S 4. Temperature changes under different voltage conditions



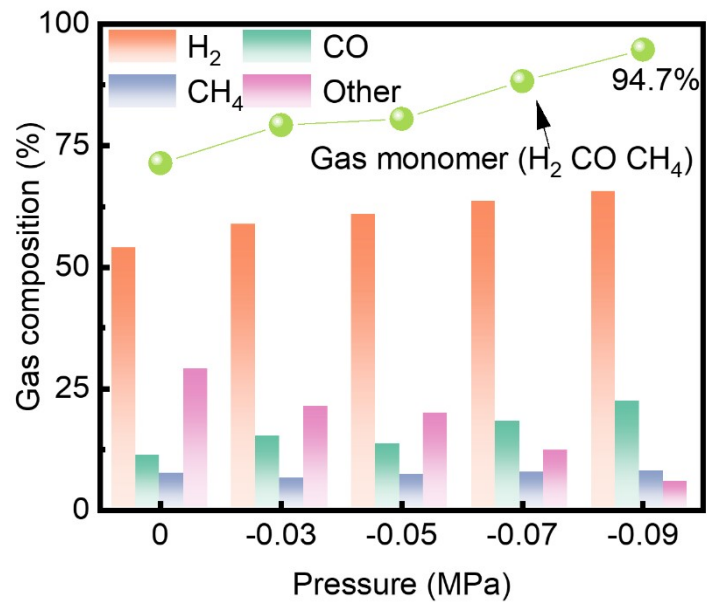
Supplementary Figure S 5. Infrared spectrum of different coal types



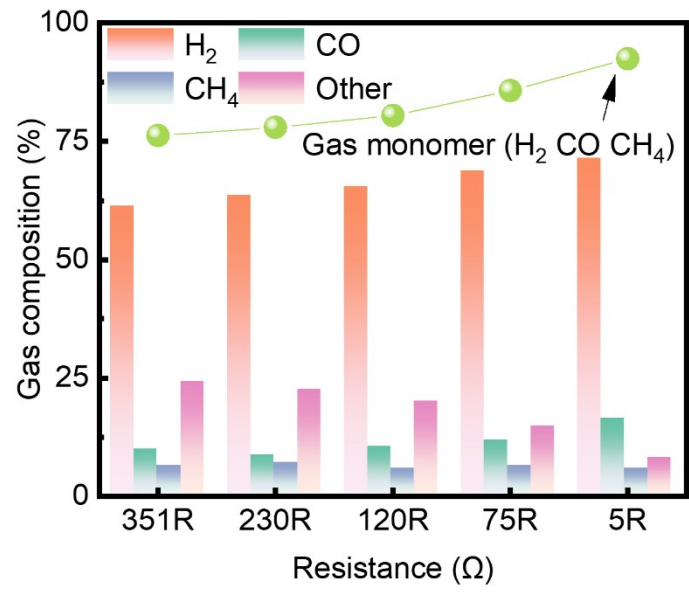
Supplementary Figure S 6. Thermal weight of different coal types



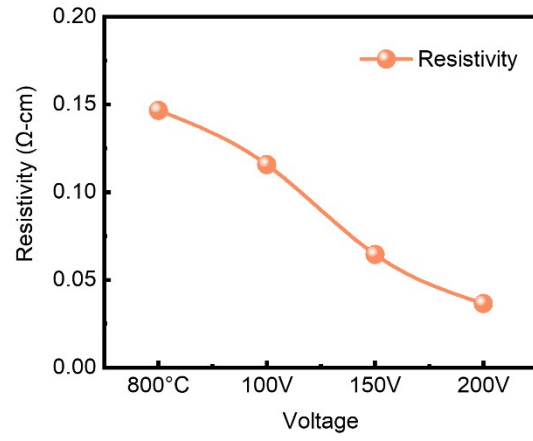
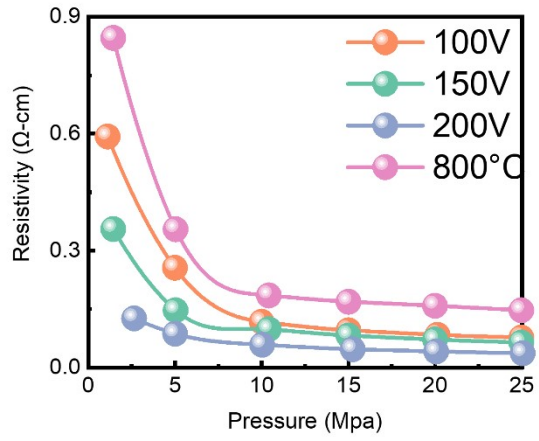
Supplementary Figure S 7. Effect of pressure on gas production



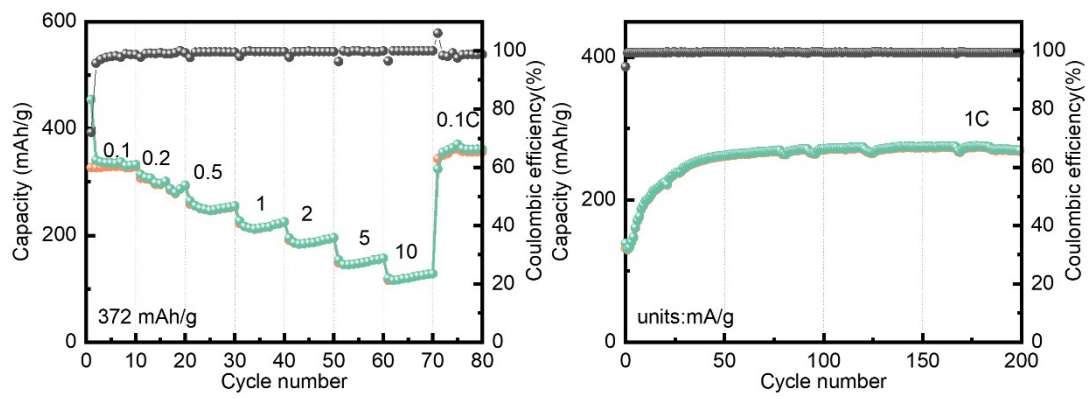
Supplementary Figure S 8. Effect of resistance on gas production



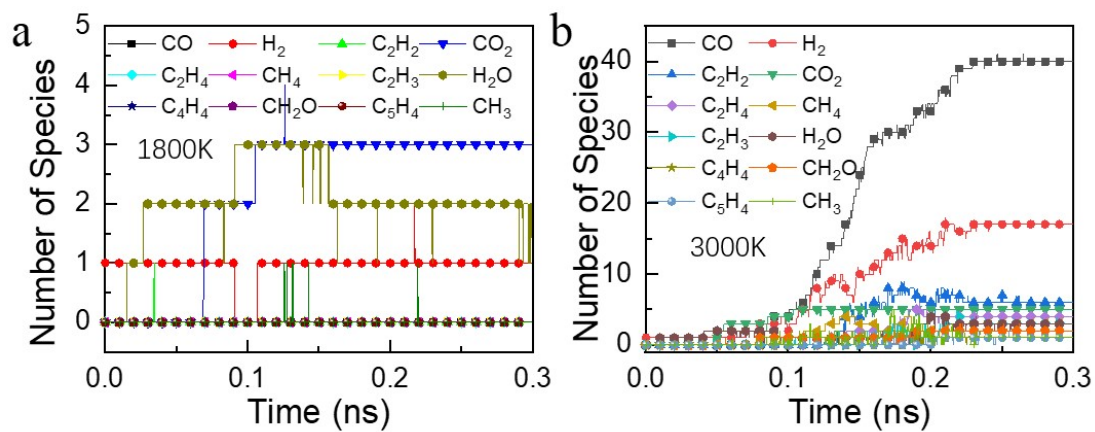
Supplementary Figure S 9. Resistivity of carbon at different voltages and slow heating



Supplementary Figure S 10. Lithium-ion battery performance



Supplementary Figure S 11. Number of species at different temperatures



Supplementary Table S1. The proximate and ultimate analyses of raw coals, wt %

Sample	proximate analyses				ultimate analyses				
	M _{ad}	A _d	V _{adf}	FC	C	H	O	N	S
Anthracite	1.54	2.86	8.76	86.84	89.64	1.15	1.25	0.54	0.07
Bituminous	7.84	1.59	31.75	58.82	71.15	6.54	7.88	1.64	1.11
Lignite	3.95	20.64	34.88	40.53	57.13	3.50	15.06	0.84	0.65

Notes: ad: air-dried basis; M: Moisture; A: Ash; V: Volatile; FC: Fixed carbon.

Industrial analysis and elemental analysis of the sample are based on GB/T 212–2008 and ash composition analysis is according to GB/T 1574–2007. The instruments for industrial analysis and elemental analysis are 5E-MAG6700 and EA 2400II, respectively. Proximate analysis results and ash compositions of the sample are shown in Tables 1.

The structure of the flash graphene model is as follows: the yellow ones at the top and bottom are copper electrodes with length of 5 mm and diameter of 6 mm; the black one in the middle is the sample with length of 5 mm and diameter of 6 mm; the thickness and length of the outer quartz tube are 1 mm and 15 mm, respectively. the initial temperature of all materials is 293.15 K.

The relevant properties of the materials are shown in the following table

Supplementary Table S2: Parameters of finite element simulation

	$\sigma /$ S/m	$C_p /$ J/(kg*K)	ϵ_r	$\rho /$ kg/m ³	$k /$ W/(m*K)
Electrodes	5.998e7	385	1	8940	400
Sample	600	710	1	1950	150
Quartz	1e-14	730	4.2	2210	1.4

The heat in the flash Joule heating process is controlled by Joule heat, and the energy transfer is in accordance with the first law of thermodynamics, which contains three ways of heat transfer: heat conduction, heat convection, and heat radiation.

The total heat transfer model is

$$\rho C_p \frac{\partial T}{\partial t} + \rho C_p \mathbf{u} \cdot \nabla T + \nabla \cdot \mathbf{q} = Q + Q_{\text{ted}} \quad (2)$$

Note: ρ is material density, C_p is constant pressure heat capacity, T is temperature, k is thermal conductivity, \mathbf{q} is thermal energy, Q is heat source, \mathbf{u} is convective heat transfer coefficient.

The Joule heat due to electrothermal coupling is controlled by the following equation:

$$\begin{aligned} \nabla \cdot \mathbf{J} &= Q_{j,v} \\ \mathbf{J} &= \sigma \mathbf{E} + J_e \\ \mathbf{E} &= -\nabla V \\ \mathbf{D} &= \varepsilon_0 \varepsilon_r \mathbf{E} \end{aligned} \quad (3)$$

Note: \mathbf{J} is the current density in A/m²; $Q_{j,v}$ is the volume loss density in W/m³; σ is the conductivity S/m, J_e is the external current density in A/m²; V is the potential in V; \mathbf{E} is the electric field in V/m; \mathbf{D} is the potential shift field in C/m²; ε_r is the relative dielectric constant; ε_0 is the relative dielectric constant.

Supplementary Table S3. Parameters for FJH

Precursors	Resistance/ Ω	Initial Voltage / V	End Voltage / V	Times / s	Energy / kJ/g
Anthracite	~300	150	80.3	0.5	8.03
Bituminous	~33	150	48.4	0.5	10.08
Lignite	~100	150	69.8	0.5	8.81
Wood	~80	150	50.2	1	9.99
Walnut shells	~91	150	77.5	1	8.25
Waste paper scraps	~274	150	77.9	4	8.22
Coffee grounds	~27	150	98.9	4	6.36
Rice husks	~69	150	28.9	4	10.83
plexiglass	~57	150	8.8	3	11.21
PVC	~29	150	41.9	4	10.37
rubber	~30	150	32.5	2	10.72

The duration mentioned refers to the time the switch is on, not the true flash duration. For amorphous non-conductive carbon sources, a common practice is to incorporate 5%-10% conductive carbon black to enhance conductivity. The sample mass used is 100 mg per batch unless otherwise specified, and the capacitance is 100 mF. Taking anthracite as an example, the initial voltage is 150 V, the end voltage is 80.3 V, and the energy supported by the material is calculated using the formula:

$$E = \frac{(V_1^2 - V_2^2) \cdot C}{2 \cdot M}$$

where: E is the energy,

V_1 is the initial voltage (150 V),

V_2 is the end voltage (80.3 V),

C is the capacitance (100 mF), and

M is the mass of the sample.

Plugging in the values, the energy supported by the material is calculated to be

8.03 kJ/g.

Supplementary Table S4. Process comparison

Technology	Heating method	Time	T/°C	Rate °C/s	Advantages	Disadvantages
Conventional pyrolysis	Radiation	Hours	<1800	5-50	simple and the cost is low	Low Recovery Rate for High-Value Products
Catalytic pyrolysis	Radiation	Hours	<1800	5-50	Catalysts increase the pyrolysis rate	Catalysts pricier, costlier, separation process complex.
Microwave pyrolysis	Dipolar molecular vibration	0.5-10s	150-600	10~200	quick, even heat distribution.	Catalyst prone to coking, affected by dielectric properties.
Plasma pyrolysis	arc heating	s	~5000	10 ⁶	Plasma boosts supercharged particles and free radicals.	The equipment is complex.
UHTFP	joule heating	ms	>3000	10 ⁵	Boosting H ₂ , Cutting CO ₂ , FG	Explore large industrial applications.

UHTFP technology represents a new and advantageous form of pyrolysis compared to traditional methods, offering several key benefits:

High Energy: Adopting the principle of FJH, UHTFP technology can rapidly heat samples to ultra-high temperatures (exceeding 3000°C) in a short duration. This high energy input facilitates the efficient destruction of chemical bonds in organic substances, surpassing the energy levels achieved by traditional pyrolysis technology.

Fast Speed: UHTFP technology completes sample pyrolysis in a few milliseconds, exhibiting a significantly faster rate compared to traditional pyrolysis methods. This accelerated process greatly enhances production efficiency.

Good Uniformity: The technology ensures even heating of the sample throughout the process, preventing issues like incomplete pyrolysis due to uneven temperature distribution, a challenge often encountered in traditional pyrolysis methods.

Good Versatility: UHTFP technology is adaptable for various pyrolysis reactions, facilitating the rapid pyrolysis of different materials. This versatility allows for the preparation of diverse high-quality chemicals, including but not limited to flash graphene.

Good Sustainability: This technology improves the efficiency and sustainability of pyrolysis reactions. With low energy consumption and the absence of the need for additional chemicals during the pyrolysis process, it reduces the overall consumption of energy and chemicals, thereby lowering costs and minimizing environmental impact.

In summary, UHTFP technology stands out for its superior energy input, rapid processing speed, uniform heating, versatility across reactions, and sustainability, making it a promising and environmentally friendly advancement in the field of pyrolysis.

Supplementary Table S5. Comparison of the UHTFP process with state-of-the-art flash pyrolysis and thermochemical systems.

Pyrolysis Technology	Feedstock	Peak Temp. (K)	Time	Main Gas Product	Main Solid Product	Ref.
UHTFP (This Work)	Coal, Biomass, Plastics	~3000	ms	94.7 vol% Combustibles	Battery-grade FG	This work
Microwave Pyrolysis	Plastics / Biomass	~1000–1200	Minutes	Mixed Syngas	Biochar	[1]
Fluidized-bed Pyrolysis	Coal / Biomass	~500–1200	1–5 s	Syngas (High CO ₂)	Biochar	[2]
Thermal Plasma	Waste Plastics	> 2000	ms	Syngas / Monomers	Carbon Black / Soot	[3]

- [1] Y. Shen. Microwave-assisted pyrolysis of biomass and plastic wastes for hydrogen production. *Green Chemistry*. **27**, 10402-10422 (2025). 10.1039/D5GC03030G
- [2] A. V. Bridgwater. Review of fast pyrolysis of biomass and product upgrading. *Biomass and Bioenergy*. **38**, 68-94 (2012). <https://doi.org/10.1016/j.biombioe.2011.01.048>
- [3] K. Sharma, M. D. Yadav, A. Sharma, S. Bhandari, S. Ghorui, et al., Engineering insights into thermal plasma processing for plastic waste management: A review. *Reviews in Chemical Engineering*. **42**, 69-111 (2026). doi:10.1515/revce-2025-0012